Applied Catalysis B: Environmental 320 (2023) 121980

Contents lists available at ScienceDirect

Applied Catalysis B: Environmental

journal homepage: www.elsevier.com/locate/apcatb

Electrogenerated quinone intermediates mediated peroxymonosulfate activation toward effective water decontamination and electrode antifouling

Fuqiang Liu [a], Zhiyuan Wang [a], Shijie You [b,*], Yanbiao Liu [a,*]

[a] College of Environmental Science and Engineering, Textile Pollution Controlling Engineering Center of the Ministry of Ecology and Environment, Donghua University, 2999 North Renmin Road, Shanghai 201620, China
[b] State Key Laboratory of Urban Water Resource and Environment, School of Environment, Harbin Institute of Technology, Harbin 150090, China

ARTICLE INFO

Keywords:
Quinone intermediates
Electrooxidation
Nonradical pathway
Water decontamination
Electrode antifouling

ABSTRACT

The activation of peroxymonosulfate (PMS) by redox-active quinones-like compounds has been proposed as a viable approach for water decontamination, which is, however, limited by the secondary pollution associated with *ex situ* addition of organic activators. Herein, we demonstrated a novel *in situ* produced quinone intermediates-mediated PMS activation technique for organic decontamination. The parent pollutant (*e.g.,* aniline) was first transformed to quinones-like intermediates by electrooxidation, followed by nucleophilic addition with PMS to initiate the production of singlet oxygen ($^1O_2$), which significantly improved the pollutant degradation and mineralization kinetics when compared to conventional electrooxidation technologies. Advanced characterizations and experimental evidence showed that the proposed method could significantly reduce electrode fouling, which is a common limitation of electrooxidation processes. The system could function efficiently across a pH range of 3–11. Experiments with genuine aniline-contaminated dyeing effluent confirmed the excellent system efficacy.

1. Introduction

On account of its high efficiency, chemical-free, and ease of process integration, electrochemical oxidation is gaining special interest as a promising decentralized water purification technique [1,2]. However, electrode fouling impedes the practical applications of this promising technique, due to the increase in ohmic resistance and overpotential caused by the formation of anodic polymeric products on electrode surface [3,4]. These polymeric intermediates are known for their large molecular size, high structural stability, and low geometric polarity, which makes them thermodynamically stable even at low anode potential [5,6]. The creation of a polymeric layer during the electrooxidation of phenol on a platinum anode, for example, resulted in a one-order-of-magnitude reduction in peak current [7]. Hence, it is highly desirable to develop advanced electrochemical oxidation system with excellent water decontamination efficacy as well as mitigated electrode fouling.

It has been well-documented that electrochemical oxidation of aromatic compounds (*e.g.,* aniline and phenol) usually leads to the formation of electro-rich intermediates [8–10], because electrons in nucleophilic C-NH_2 or C-OH can be readily transferred to C═O and C-$O^{\bullet}$. Among them, quinone intermediates are redox-active species because of their high electron density and strong electron-donating properties [11,12]. They can be used as metal ligands and/or reductant in environmental geochemistry to promote transition-metal redox cycling in natural organic materials [13–16]. Due to the facilitated circulation of Fe(III)/Fe(II) couples, it has been established that the presence of quinones-like compounds can considerably increase the Fenton reaction activity [17].

Inspired by these findings, some research groups have used quinones (*e.g., p*-benzoquinone (BQ)) as metal-free organic activators for peroxymonosulfate (PMS) toward water purification [18,19]. For example, Zhou et al. [20] found that the interaction between BQ (10 μM) and PMS could degrade sulfamethoxazole (8 μM) by up to 86% within 3 min (0.44 mM). Zhang et al. [21] also found that halogenated and methylated quinones (*e.g.,* 2,6-dimethyl-1,4-benzoquinone and 2,6-dichloro-1,4-benzoquinone) could efficiently activate PMS, and the process was pH and quinones dependent. In addition, the BQ can catalyze singlet oxygen

* Corresponding authors.
E-mail addresses: sjyou@hit.edu.cn (S. You), yanbiaoliu@dhu.edu.cn (Y. Liu).

https://doi.org/10.1016/j.apcatb.2022.121980
Received 18 February 2022; Received in revised form 9 September 2022; Accepted 11 September 2022
Available online 13 September 2022

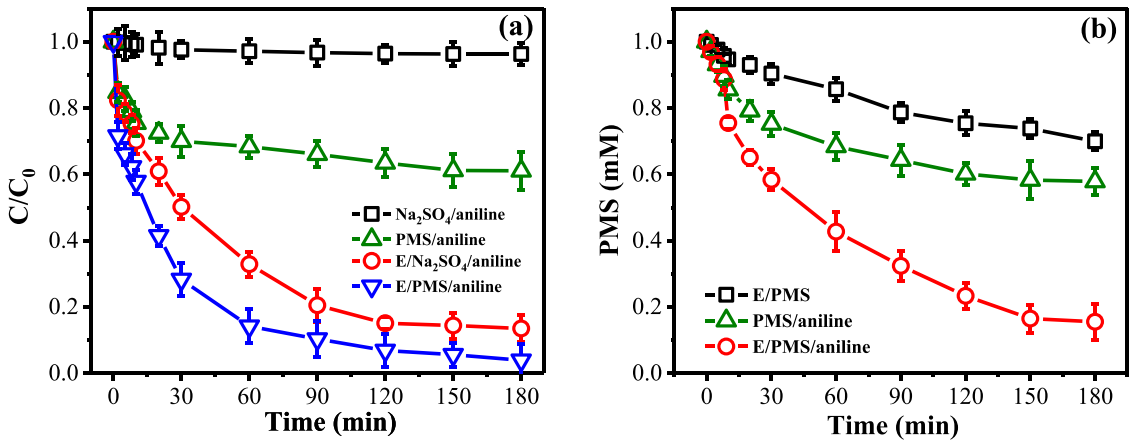

Fig. 1. (a) Degradation of aniline in different systems with time. (b) Change of PMS concentration with time in different systems. Experimental conditions: $[aniline]_0$ = 50 mg/L, $[PMS]_0$ = 1.0 mM, applied potential = 1.2 V and pH_0 = 6.5.

($^1O_2$) generation with almost 100% selectivity through a cascade of events involving nucleophilic addition of PMS, displacement, and breakdown of the essential dioxirane intermediates, according to accumulating data [20–22]. Because $^1O_2$ offers unique characteristics such as a wide pH tolerance and great selectivity, these desirable characteristics may offer new avenues toward effective water decontamination [23–25]. Furthermore, $^1O_2$ might be used instead of radicals to selectively oxidize a range of electron-rich pollutants even in the presence of complex organic matters [26–28]. However, the *ex situ* introduction of organic activators would result in substantial secondary contamination, making practical uses in water cleanup difficult.

In this paper, our goal is to build a novel *in situ* PMS activation system for water purification triggered by the formation of electrogenerated quinones. Aniline, a common contaminant in industrial effluent, was chosen as a model contaminant. We anticipate that polymeric quinones intermediates might be produced *in situ* by electrochemical anodic oxidation of aniline, followed by activation of PMS to produce reactive $^1O_2$, which could then be used to degrade leftover aniline and other organic polymeric intermediates. This method will not only avoid the need for additional activators, making PMS activation more cost-effective and long-term, but also address electrode fouling in electrochemical oxidation. The paper is consisted of the following sections. First, the electrochemical degradation of aniline was assessed and compared in a variety of operating environments. Second, using chemical quenching and trapping methods, the major reactive species within the electrochemical PMS activation (E/PMS/aniline) system were identified, and the production process of $^1O_2$ was explained based on experimental evidence and theoretical calculations. Third, the E/PMS/aniline system was used to test the electrode antifouling capability. Fourth, the effects of several key factors (*e.g.,* aniline concentration, applied potential, solution pH, and PMS concentration) on aniline degradation kinetics were investigated and optimized. Finally, the good application potential of the proposed electrochemical technology was assessed.

2. Experimental section

2.1. Chemicals

All chemicals employed were analytical grade and had not been further purified. Carbon nanotubes (CNT) with many walls were obtained from TimesNano Co., Ltd (Chengdu, China). Aniline (C_6H_7N, 99.5%), peroxymonosulfate (PMS, $KHSO_5{\cdot}0.5KHSO_4{\cdot}0.5K_2SO_4$, 98.0%), 2,2,6,6-tetramethyl-4-piperidinol (TEMP, $C_9H_{19}N$, 96.0%), 5,5-dimethyl-1-pyrroline-n-oxide (DMPO, 97.0%) and tin chloride dihydrate ($SnCl_2{\cdot}2H_2O$, 98.0%) were purchased from Sigma-Aldrich (St. Louis, MO). Sodium sulfate (Na_2SO_4, 99.0%), benzoic acid ($C_7H_6O_2$, 99.5%), n-methyl-2-pyrrolidinone (NMP, 99.5%), hydrochloric acid (HCl, 36.0–38.0%), sodium hydroxide (NaOH, 96.0%), furfuryl alcohol (FFA, $C_5H_6O_2$, 98.0%), methanol (CH_3OH, 98.0%), sodium thiosulfate pentahydrate ($Na_2S_2O_3{\cdot}5H_2O$, 99.0%) and ethanol (C_2H_5OH, 96.0%) were obtained from Sinopharm Chemical Reagent Co., Ltd. Stock solutions were produced by ultrapure water (18.25 MΩ cm) obtained from a Milli-Q Direct 8 water purification system (Millipore, USA).

2.2. Experimental setup and operational procedures

The preparation of the SnO_2-CNT electrode used in this study has been described in previous work [29], and the morphology of the SnO_2-CNT anode is shown in Fig. S1. Electrochemical experiments were performed on an electrochemical workstation (CHI 760E, Chenhua) in a cylindrical three-electrode single-compartment cell with a high-stability SnO_2-CNT working electrode, a Ti sheet counter electrode, and a saturated Ag/AgCl reference electrode. Typically, 100.0 mL PMS aqueous solution containing 50 mg/L aniline was electrolyzed in a 120.0 mL electrochemical cell, which was continuously stirred by a magnetic stirrer at 500 rpm. Sodium sulfate (1 mM) was added to the solution as a background electrolyte. On the aniline degradation performance, the influences of applied potential (0.8–1.4 V), initial PMS concentration (0.5–1.5 mM), and solution initial pH (3–11) were examined. Solution pH was adjusted by 1 M NaOH and/or HCl. Samples of 2.0 mL were taken regularly and were mixed with 0.1 mL of 50 mM $Na_2S_2O_3$ to quench the degradation reaction. Aniline and BQ was quantified using a Waters 3000 system with a UV detector for high-performance liquid chromatography (HPLC). Intermediates were identified with gas chromatography coupled with mass spectrometry (GC-MS) on an Agilent 7890A-5975 C. All of the degradation tests were performed three times and the mean values with standard deviation were provided.

2.3. Characterizations

A field emission scanning electron microscope (FESEM, S-4800, Japan) was used to examine the morphology of the as-fabricated SnO_2-CNT electrode. X-ray photoelectron spectroscopy (XPS) was conducted in a Thermo Fisher Scientific Escalab 250Xi (USA) under high vacuum (1×10^{-9} Torr), and all binding energies were calibrated to the C 1 s peak at 284.8 eV. Fourier transform infrared spectroscopy (FTIR, Tensor27) was used to study the surface structure of the SnO_2-CNT electrode. The oxidizing species were detected using a Bruker EMXnano electron paramagnetic resonance (EPR) spectrometer, with DMPO and TEMP as radical trapping agents. For all tested systems, 200 μL reaction solution was immediately added into the 10 μL trapping agent after 20

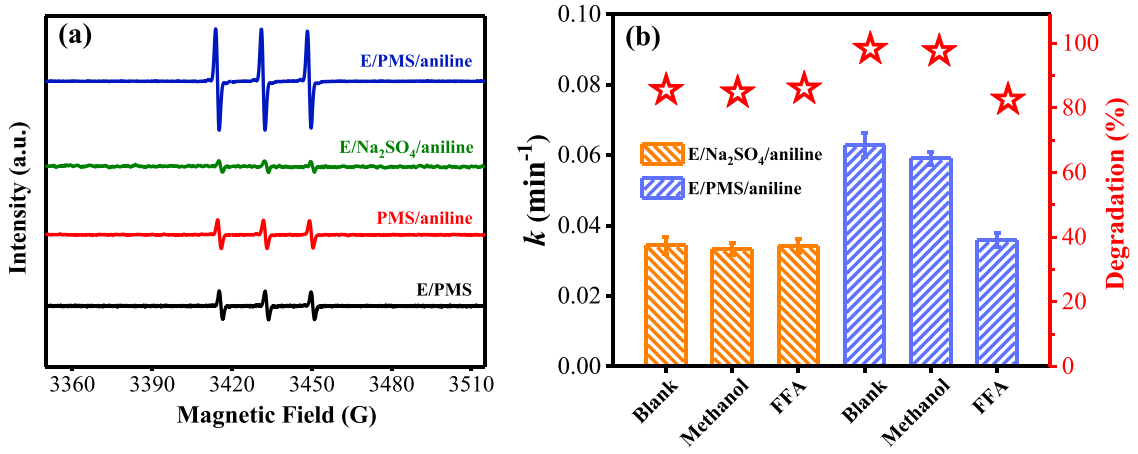

Fig. 2. (a) EPR spectra for the detection of $^1O_2$ in the presence of TEMP under different operating systems. (b) Comparison of aniline degradation performance between E/Na_2SO_4/aniline and E/PMS/aniline systems in the presence of different radical scavengers including methanol (100 mM) and FFA (50 mM). Experimental conditions: $[aniline]_0$ = 50 mg/L, $[PMS]_0$ = 1.0 mM, applied potential = 1.2 V and pH_0 = 6.5.

min of operation. The mixture was sampled by a 100 μL capillary tube, which was inserted into the EPR cavity. The EPR spectra were obtained at room temperature with a center field of 3430 G, a sweep width of 200 G, a sweep time of 30 s, a modulation amplitude of 5 G, a microwave power of 10 mW and a modulation frequency of 100 kHz. Mineralization was determined by total organic carbon (TOC, Vario TOC cube, Elementar). Electrochemical impedance spectroscopy (EIS) measurements were performed using a CHI 660E electrochemical workstation (Shanghai, China) over the frequency range from 100 kHz to 0.1 Hz at an amplitude of 5 mV.

2.4. Theoretical calculations

Theoretical insights into the degradation mechanism related to PMS activation by quinones intermediates and aniline degradation were studied using density functional theory (DFT) simulations. The B3LYP/6–31 G(d) level was used for geometry optimizations and frequency calculations.

3. Results and discussion

3.1. Electrochemical degradation of aniline

Several control experiments were carried out at pH 6.5 to show the benefits of electrochemical aniline degradation in the presence of 1 mM PMS (E/PMS/aniline) (Fig. 1a). As could be observed, physical adsorption of aniline by a SnO_2-CNT electrode could be ignored after 180 min (<5%, black line). Additionally, it was discovered that in the presence of PMS alone (PMS/aniline), around 40% of aniline was destroyed. This slightly effective performance was comparable to the preceding report [30], which is mainly due to the direct oxidation of PMS (1.75–1.82 V *vs.* NHE) and a small amount of $^1O_2$ produced by self-decay of PMS (k = 0.2 M^{-1} s^{-1}, Eq. (1)) [20]. When the applied potential of 1.2 V, aniline could be obviously degraded by anodic oxidation with an equal amount of Na_2SO_4 as electrolyte (E/Na_2SO_4/aniline). It is well-known that aromatic pollutants can be degraded by direct electron transfer or surface-bound reactive oxygen, accompanied by the generation and accumulation of high-resistance polymeric intermediates [5]. In contrast, when PMS was used instead of Na_2SO_4 to build the E/PMS/aniline system, aniline degradation was significantly accelerated. The degradation efficiency of aniline increased from 86.5% to 96.1% and the corresponding first-order kinetic constant (k) increased from 0.034 min^{-1} to 0.063 min^{-1} (R^2 > 0.98). More importantly, the deduction in TOC in the E/PMS/aniline system (71.1%) showed a significant enhancement compared to the E/Na_2SO_4/aniline (40.2%) and PMS/aniline (7.6%) systems (Fig. S2). These phenomena indicated that the presence of PMS in E/PMS/aniline system had unique superiority in promoting aniline degradation and mineralization.

$$HSO_5^- + SO_5^{2-} \rightarrow HSO_4^- + SO_4^{2-} + {}^1O_2 \quad (1)$$

To visually highlight the role of PMS in the oxidation process, the residual contents of PMS were monitored and compared as a function of time in three different systems (Fig. 1b). The concentration of PMS steadily dropped with time in the PMS/aniline process, with a final consumption of ~40%, which might be attributed to the causes indicated above and was consistent with the limited degradation performance (Fig. 1a). There was a much slower decline (<30%) in the E/PMS system due to the electro-activation of PMS [31]. By comparison, the reduction in PMS concentration was quick for the E/PMS/aniline procedure, and it was lowered by around 80% after 180 min. Based on these observations, the PMS consumption in the E/PMS/aniline system was higher than the sum of PMS consumption of the other two systems, inferring that there might be other pathways exist in the E/PMS/aniline system to rapidly and efficiently decompose PMS.

3.2. Identification of reactive species

To demonstrate the beneficial effect of PMS on the electrochemical breakdown of aniline, EPR technique was used to identify the active species, with DMPO and TEMP serving as spin trapping agents. Generally, $HO^•$, $SO_4^{•-}$ and $^1O_2$ are considered to be the oxidizing species in the degradation processes of pollutants involving PMS. Based on this, DMPO was first employed to verify the formation of $HO^•$ and $SO_4^{•-}$, however, none of the tested systems showed any characteristic peak (Fig. S3). To confirm this result, the methanol, as the common radical quencher for $HO^•$ ($k = 9.7 \times 10^8$ M^{-1} s^{-1}) and $SO_4^{•-}$ ($k = 3.2 \times 10^6$ M^{-1} s^{-1}) [32], was added to the solution with an excess concentration of 100–1000 mM. In the E/PMS/aniline and E/Na_2SO_4/aniline systems, there was essentially no influence on aniline degradation (Figs. 2b and S4). To further verify this, benzoic acid (BA) was employed as another quencher of $HO^•$ ($k = 6.0 \times 10^9$ M^{-1} s^{-1}) and $SO_4^{•-}$ ($k = 1.2 \times 10^9$ M^{-1} s^{-1}) [33]. Consistently, with an increased dosage of BA from 0 to 10 mM, only a negligible change in the aniline degradation was identified (Fig. S5). These provided solid evidence that neither $HO^•$ nor $SO_4^{•-}$ was dominant in the E/PMS/aniline and E/Na_2SO_4/aniline systems.

Importantly, when TEMP was utilized as the $^1O_2$ trapping agent, the characteristic triplex peak signal (1:1:1) of the TEMP-$^1O_2$ adduct was observed in all cases, with a considerable variation in signal amplitude (Fig. 2a). A faint EPR signal was recorded in the E/Na_2SO_4/aniline system, which could be attributed to the presence of extremely minute

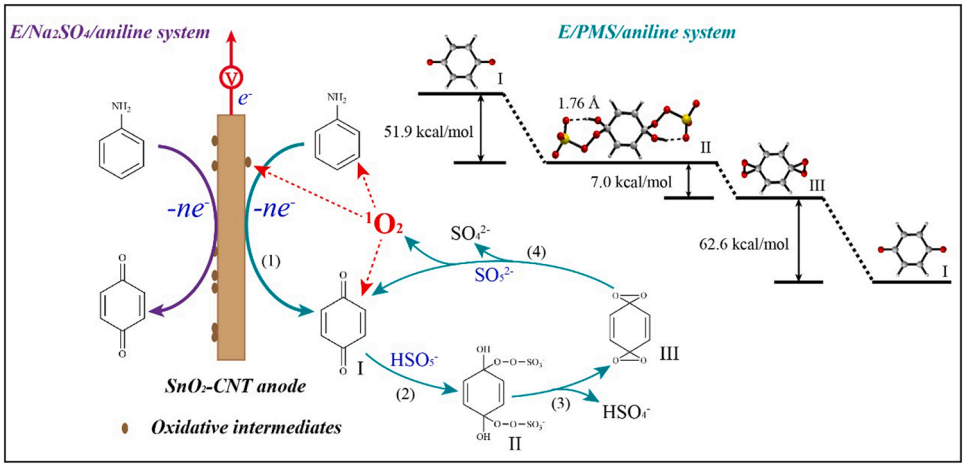

Fig. 3. Proposed possible mechanism for $^1O_2$ production and relevant free energy diagram in the *in situ* organic quinones-mediated PMS activation system.

amounts of $^1O_2$ from the ultrapure water [34]. While in the E/PMS and PMS/aniline systems, the EPR signal with a slight improvement may primarily derive from the self-decomposition of PMS and the reaction between PMS and aniline [18], which could slowly generate $^1O_2$. In contrast to other systems, the E/PMS/aniline process generated a strong EPR peak intensity, implying that the high yield of $^1O_2$ required the joint action of applied potential, PMS, and aniline. In other words, the anodic oxidation intermediates of aniline served as the main activator for the disintegration of PMS. As a result, $^1O_2$ is anticipated to cause increased aniline degradation and mineralization in the E/PMS/aniline system. EPR analysis was also used to determine the concentration of $^1O_2$ in various systems [35]. As presented in Fig. S6, the concentration of $^1O_2$ produced by the E/PMS/aniline system was as high as 105.2 μM, which was in sharp contrast to 2.68 μM from E/Na_2SO_4/aniline, 11.5 μM from PMS/aniline, and 10.6 μM from E/PMS. This was consistent with the above degradation performance of aniline (Fig. 1a).

Furthermore, to show the role of $^1O_2$, FFA was dosed (50 mM) as a typical scavenger for eliminating $^1O_2$ ($k = 1.2 \times 10^8$ M^{-1} s^{-1}) [36]. As demonstrated in Fig. 2b, adding FFA to the E/Na_2SO_4/aniline system failed to affect aniline degradation, however, adding FFA to the E/PMS/aniline system resulted in an evident decline in the aniline degradation kinetics from 0.063 min^{-1} to 0.036 min^{-1}. Meanwhile, the degradation (82.5% *vs.* 86.5%) and mineralization (37.6% *vs.* 40.2%) after inhibition was identical to that of the E/Na_2SO_4/aniline system, which can be attributed to the similar electrooxidation routes. To further confirm the role of $^1O_2$, the aniline degradation was performed by changing the solvent of H_2O with D_2O, since the physical quenching of $^1O_2$ in H_2O ($k_d(H_2O) = 2.5 \times 10^5$ s^{-1}) was faster than that in D_2O ($k_d(D_2O) = 1.5 \times 10^4$ s^{-1}) [37]. As shown in Fig. S7, the degradation rate of aniline in D_2O (0.117 min^{-1}) had a significant increase compared with in H_2O (0.063 min^{-1}). This provided solid evidence on the effect of $^1O_2$ and the longer lifetime of $^1O_2$ triggered better degradation rate. The above results indirectly confirmed that the aniline degradation in the E/PMS/aniline system was mainly originated from anodic oxidation as well as the oxidation by $^1O_2$. In addition, the contribution from these two parts on the decontamination of aniline could be distinguished according to the scavenging results. The degradation of aniline declined from 96.2% to 82.5% once $^1O_2$ was quenched in the E/PMS/aniline system, suggesting that the anodic oxidation and organic Fenton-like process contributed 85.8% and 14.2% to the aniline degradation, respectively. Under similar conditions, the aniline mineralization also decreased from 71.1% to 37.6% in the E/PMS/aniline system, indicating that the contribution of anodic oxidation and organic Fenton-like process to aniline mineralization was 52.9% and 47.1%, respectively. Thus, in contrast to the E/Na_2SO_4/aniline system that depended simply on electrooxidation to degrade aniline, the E/PMS/aniline system is thought to have profited from the additional creation of $^1O_2$, which improved aniline breakdown and mineralization.

3.3. Generation and oxidation mechanisms of singlet oxygen

Previous research has shown that redox-active ketones or BQ with two carbonyl groups can catalyze PMS to create $^1O_2$ by a sequence of reactions including nucleophilic addition, displacement, and breakdown [20]. Fortunately, it has been discovered that electrooxidation process of aniline is usually accompanied by the formation of BQ and its polymers [9,38]. Thus, a comparable pathway for the generation of $^1O_2$ may exist in the E/PMS/aniline system (Fig. 3). The anodic conversion of aniline to intermediates I, such as BQ and other organic polymers owning a lot of redox-active quinone-like moieties, should be the initial step (step 1). The nucleophilic addition of PMS to the carbonyl group of intermediates I resulted in the generation of intermediates II, a peroxide adduct (step 2). With the removal of HSO_4^-, the intermediates II could be transformed to a dioxirane intermediates III (step 3). Finally, two molecules of ionized PMS ions (SO_5^{2-}) might attack the intermediates III, producing $^1O_2$ and reforming BQ (step 4). Through the oxidation of $^1O_2$, polymeric intermediates and aniline could also be further degraded to speed up and improve water purification. The existence of these reactions (steps 2–4) underscored a fundamental difference from the E/Na_2SO_4/aniline system.

GC-MS was used to identify the intermediates of the E/PMS/aniline system, which helped to confirm the suggested pathways outlined above. As shown in Fig. S8, the presence of step 1 was confirmed by the detection of BQ and its electrooxidation precursors (*e.g.,* hydroquinone) during the reaction process. Also, the aniline solution changed color from colorless to yellowish brown as electrooxidation progressed with aniline degradation, which was attributed to the production of BQ (Fig. S9). In addition, derivatives of the essential dioxirane intermediates III were discovered (Fig. S8), demonstrating the validity of the hypothesized pathways to a great extent. Unfortunately, the as-generated reactive intermediates II could not be detected using currently available tandem mass spectrometry and gas chromatography due to its poor stability and rapid consumption, a similar problem was also reported in prior research [6].

To proof the concept of quinone intermediates induced PMS decomposition to produce $^1O_2$, the relationship between aqueous BQ concentration and $^1O_2$ yield was investigated in the E/PMS/aniline system by changing the initial aniline concentration (10–100 mg/L). Results suggested that both BQ concentration (Fig. S10a) and $^1O_2$ EPR signal (Fig. S10b) enhanced with the increase of aniline concentration. A linear relationship between the $^1O_2$ yield and the BQ concentration (R^2 = 0.972, Fig. S10c) can be identified, revealing that quinones

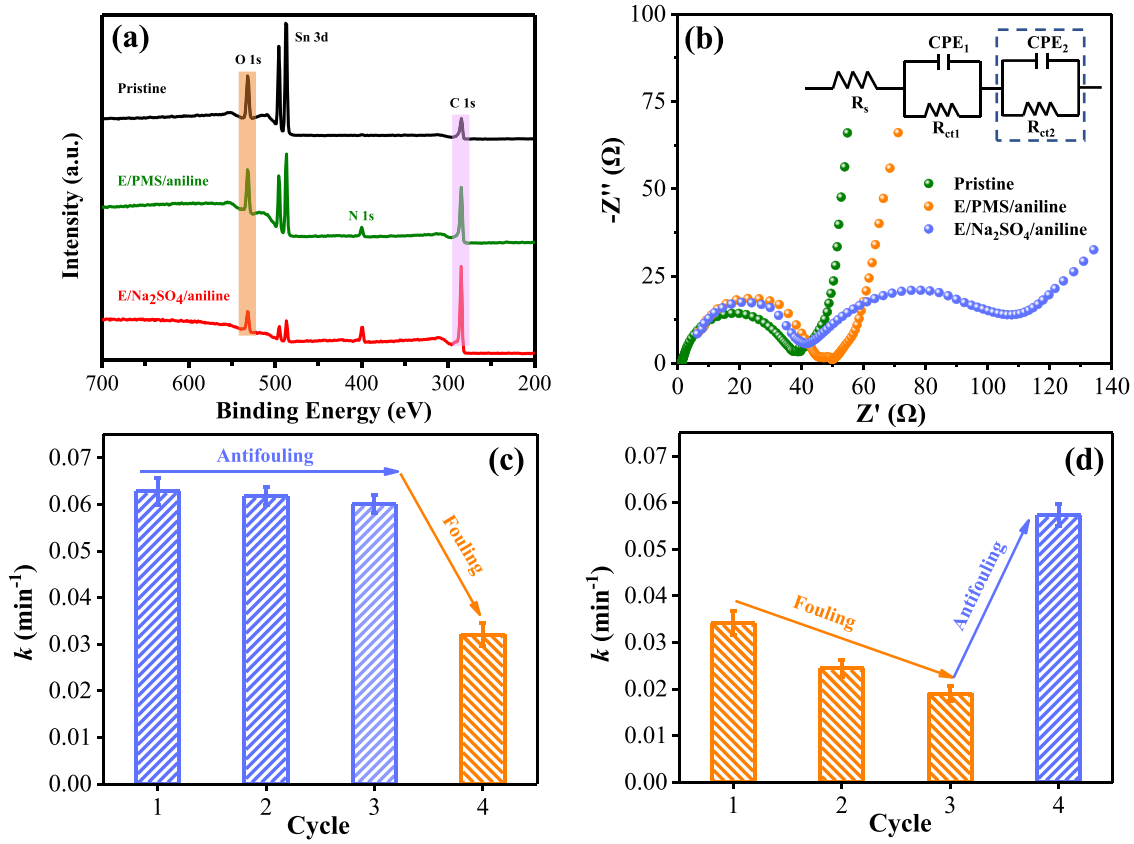

Fig. 4. Comparison of (a) XPS survey patterns and (b) Nyquist plots of the SnO_2-CNT anode in the pristine, E/Na_2SO_4/aniline and E/PMS/aniline systems. (c-d) Cyclic aniline degradation on the SnO_2-CNT anode in the E/Na_2SO_4/aniline (orange color) and E/PMS/aniline (blue color) systems. Experimental conditions: $[aniline]_0 = 50$ mg/L, $[PMS]_0 = 1.0$ mM, applied potential = 1.2 V and $pH_0 = 6.5$.

intermediates played a key role in the generation of $^1O_2$. Furthermore, previous reports showed that the electrooxidation intermediates of aniline mainly include azobenzene, nitrobenzene, quinones, phenols, short carboxylic acids and polyaniline [9,39–41], among which only quinones have been reported to possess the ability of PMS activation [18,20,21]. Thus, it can be inferred that the generated quinone intermediates were indispensable for the production of $^1O_2$ in the proposed E/PMS/aniline system.

The rationality of $^1O_2$ generation was further demonstrated using a Gaussian program and density functional theory (DFT) computations. The results revealed that the computed Gibbs free energy for each phase (steps 2–4) was negative (Fig. 3), indicating that these processes were thermodynamically favorable. Notably, our postulated pathways appeared to be at odds with prior research that found the conjugate base of intermediates II was involved in the conversion of intermediates II to III [20]. The conjugate base of intermediates II was unlikely to exist fundamentally during geometry optimization, according to DFT calculations. Due to the high electrostatic repulsive contact between the oxygen cation and peroxydisulfate anion, both of which were linked to the same C(sp3) atom, it might be considered as an exceedingly unstable intermediates. Instead, when the protonated oxygen anion in intermediates II formed an intramolecular hydrogen bond with the peroxydisulfate anion, a more stable 7-member ring was formed. Of note, the generation mechanisms of $^1O_2$ did not involve the conversion of oxygen (Fig. S11) as well as the disproportionation of superoxide radical that could be effectively quenched by the generated BQ ($k = 2.9 \times 10^9$ M^{-1} s^{-1}) [42]. Overall, based on the available data and prior discussion, a feasible PMS activation system triggered by the redox-active anodic quinones intermediates for electrochemical water purification was proposed (Fig. 3).

3.4. *In situ* electrode antifouling

When a low potential is given to an electrooxidation system, electrode fouling is the principal bottleneck, resulting in low current efficiency and excessive energy usage [43]. The key mechanisms for generating polymeric intermediates on the electrode surface are electron transfer, hydrogen abstraction, and radical complexion [6]. The electrode fouling in the E/Na_2SO_4/aniline and E/PMS/aniline systems were examined and compared in this study. As shown in Fig. 4a, the atomic percentage ratio of C/O of the electrode grew dramatically from 1.33 (pristine) to 9.32 when the electrode was utilized in the E/Na_2SO_4/aniline system. The ratio in the E/PMS/aniline system, on the other hand, only improved to 2.08 due to the elimination of organic intermediates such as phenol and quinone. This phenomenon was further confirmed by using FTIR analysis to compare the functional groups of the electrode surface (Fig. S12). In comparison to the original electrode, the surface function groups of the electrode were practically unchanging in the E/PMS/aniline system. Nevertheless, the peak of C-O-C at ~1038 cm^{-1} and ~1100 cm^{-1} was emerged in the E/Na_2SO_4/aniline system [44]. Also, the IR adsorption increased at ~1740 cm^{-1} and ~1640 cm^{-1}, which could be attributed to the quinone (C═O) and residual of acid (COOH) or alcohol groups (C-OH), respectively [45]. Furthermore, the EIS was also used to investigate electrode fouling, which was particularly useful for the non-conductive fouling film (Fig. 4b). The electrode utilized in the E/Na_2SO_4/aniline system included two semicircular loops in the mid-frequency and low-frequency regions, which indicated charge transfer impedance (R_{ct}, 40.2 Ω) and interface resistance (67.4 Ω), respectively, on Nyquist plots. This result showed the formation of a new interface between the SnO_2-CNT electrode and electrolyte [7]. The reduced resistance (63.4 Ω) suggested that the E/PMS/aniline system might considerably mitigate electrode fouling when compared to

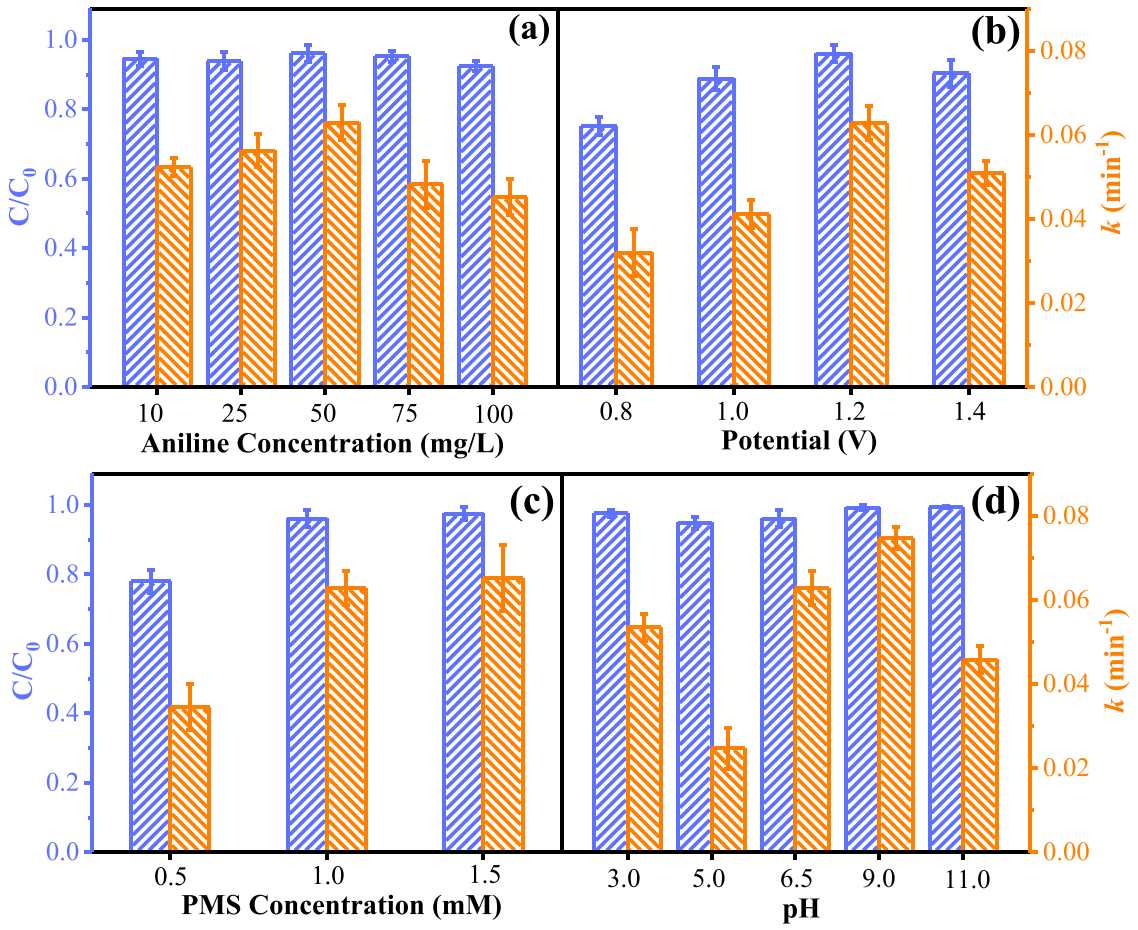

Fig. 5. Effects of (a) initial aniline concentration (applied potential = 1.2 V, $[PMS]_0$ = 1.0 mM and pH_0 = 6.5), (b) applied potential ($[aniline]_0$ = 50 mg/L, $[PMS]_0$ = 1.0 mM and pH_0 = 6.5), (b) PMS concentration ($[aniline]_0$ = 50 mg/L, applied potential = 1.2 V and pH_0 = 6.5) and (c) initial pH ($[aniline]_0$ = 50 mg/L, $[PMS]_0$ = 1.0 mM and applied potential = 1.2 V) on the aniline degradation in the E/PMS/aniline system.

the electrode used in the E/PMS/aniline system (44.2 Ω), which was close to the fresh electrode (37.9 Ω).

Furthermore, to better show the advantages of self-cleaning electrode used in the E/PMS/aniline system, cyclic aniline degradation tests were carried out by using the same electrode (Fig. 4c). The degradation rates (0.060–0.064 min^{-1}) of three consecutive cycles were similar in the E/PMS/aniline system, according to the results. However, when Na_2SO_4 was used instead of PMS for the fourth run, the rate would drop dramatically (0.032 min^{-1}). In comparison, the degradation of aniline in the E/Na_2SO_4/aniline system presented a continuous downward trend (from 0.034 min^{-1} to 0.019 min^{-1}) due to the accumulation of intermediates polymers incessantly on the electrode. This worsening could be restrained and even greatly improved (0.057 min^{-1}) when PMS was added in the fourth cycle (Fig. 4d). These results demonstrated that an *in situ* organic mediated PMS activation system might not only increase electrochemical water purification but also achieve *in situ* electrode antifouling.

3.5. Effects of operating parameters

The effects of the initial aniline concentration, applied potential, PMS concentration, and initial pH on the breakdown of aniline were investigated to optimize the E/PMS/aniline system. Since the quinone intermediates were derived from anodic oxidation of aniline, the initial aniline concentration was considered as a sensitive factor in the electrochemical system. Results indicated that aniline could be effectively degraded (>95%) regardless of the initial aniline concentration (10–100 mg/L, Fig. 5a). Meanwhile, an inverted V-shaped relationship was observed in the aniline oxidation process (0.045–0.062 min^{-1}), where the degradation kinetics maximized at an optimum aniline concentration of 50 mg/L. This suggested that a higher aniline concentration would deteriorate the reaction kinetics in the E/PMS/aniline system, although more quinone intermediates and $^1O_2$ could be produced (Fig. S10).

The production of quinone intermediates was directly correlated with the applied potential. As seen in Fig. 5b, the E/PMS/aniline system showed enhanced activity as the potential increased from 0.8 to 1.2 V at pH 6.5. The aniline degradation efficiency was found to be 75.2%, 88.9%, and 96.1%, respectively, with corresponding *k* values of 0.032, 0.041, and 0.063 min^{-1}. This could be expected because when the applied potential was increased, more BQ could be generated and resulted in more $^1O_2$ being produced, thus speeding up the aniline degradation. Nevertheless, a further increase in the potential to 1.4 V yielded less efficient aniline degradation (90.5% and 0.051 min^{-1}), possibly since the oxygen evolution began to occur [46]. Therefore, the applied potential was fixed at 1.2 V for the subsequent investigations.

Following that, the effect of various PMS dosages ranging from 0.5 m to 1.5 mM on aniline degradation was investigated. As shown in Fig. 5c, the degradation performance increased gradually with the increased dosage of PMS. Although the optimal activity was at a dosage of 1.5 mM PMS, there was only a slight improvement compared to the 1.0 mM PMS (96.1% *vs.* 97.5%, 0.063 min^{-1} *vs.* 0.065 min^{-1}). To optimize the benefit, the PMS concentration of 1.0 mM was chosen as the most appropriate dosage.

The aniline degradation performance was also investigated as a function of solution initial pH (Fig. 5d). The *in situ* organic-mediated

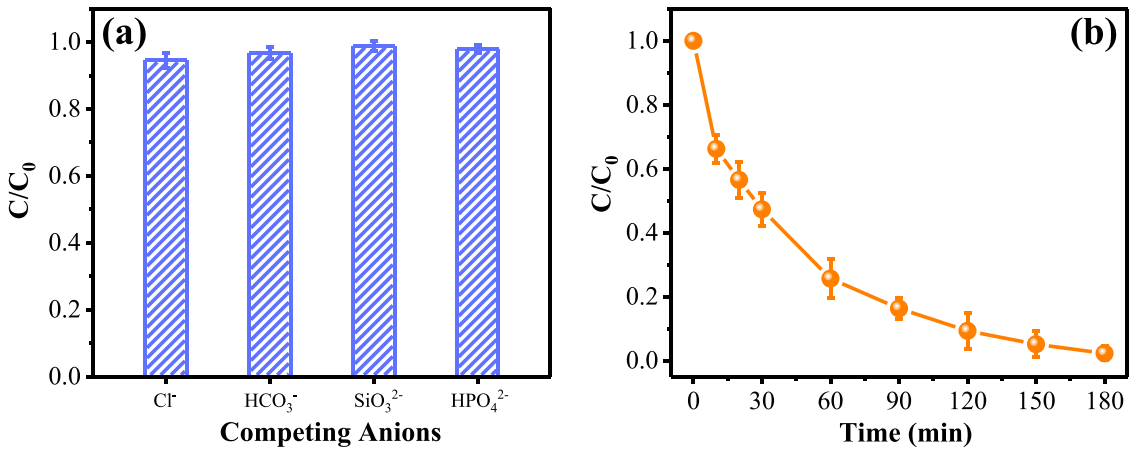

Fig. 6. (a) Effect of competing anions on the aniline degradation in the E/PMS/aniline system ([aniline]$_0$ = 50 mg/L, [competing anions]$_0$ = 10 mM, [PMS]$_0$ = 1.0 mM, applied potential = 1.2 V and pH$_0$ = 6.5). (b) The degradation of aniline when confronted with actual aniline-contaminated dyeing wastewater ([aniline]$_0$ = ~15 mg/L, pH$_0$ = 7.8).

PMS activation system could work efficiently (>90%) in a wide pH range of 3–11, demonstrating a significant advantage over typical Fenton-like reactions that prefer acidic environments. Furthermore, at varied pH circumstances, the changes in reaction rates were irregular, which could be due to the synergistic influence of multiple factors. First, because aniline has a p*K*a value of 4.6 [47], when the solution pH is near neutral or alkaline, the aniline is more likely to be transformed to quinones on the anode surface by electron transfer due to electrostatic attraction. Second, the PMS has been reported to exist mostly as HSO_5^- in acidic and neutral environments, implying that an alkaline environment may limit the formation of $^1O_2$ due to a lack of HSO_5^- [48]. Third, a recent kinetic model suggested that BQ-mediated breakdown of PMS was more likely to occur under alkaline circumstances [20]. A similar experimental phenomenon had been reported for the decomposition of phenol in a recent paper [6]. Overall, the E/PMS/aniline system demonstrated a wide pH tolerance, owing to the combined effect of the applied electric field and the metal-free organic activator produced *in situ*. In addition, Table S1 compared the aniline oxidation kinetics as a function of operational parameters in the E/PMS/aniline system.

3.6. Evaluation of system efficacy toward practical application

Despite the positive findings obtained in the lab-scale test, this is far from a realistic scenario in which wastewater is created by dyeing industries from an engineering standpoint. As a result, we first examined the aniline degradation in the E/PMS/aniline system in the presence of common anions (*e.g.,* Cl^-, SiO_3^{2-}, HCO_3^-) with an initial concentration of 10 mM. These anions exerted an almost negligible influence on aniline degradation (Fig. 6a). We further explored the potential practical application of the proposed technology by challenging the actual aniline-containing dyeing wastewater (Fig. 6b). The results indicated that the E/PMS/aniline system could achieve the degradation of 97.6% aniline (~15 mg/L) within 180 min, which suggested a great potential for application in real wastewater treatment.

4. Conclusions

This research had designed and demonstrated a unique *in situ* organic quinones-mediated PMS activation system for organic decontamination *via* a nonradical pathway, where reactive $^1O_2$ was involved. The synergy of anodic oxidation with organic Fenton-like technology might provide a larger catalytic capacity, better cyclic stability, and preferentially towards electron-rich compounds as compared to traditional electrooxidation technology. Meanwhile, this coupled system shall provide a comprehensive understanding of *in situ* electrode antifouling for organic pollutant electrooxidation. More importantly, this proposed approach not only works well in a pH range of 3–11, but also presents a good application potential when it comes to dyeing wastewater with complicated compositions. This work may provide a new opportunity to develop an efficient, robust, and cost-effective strategy for water decontamination.

The crucial metal-free redox-active organic intermediates (*e.g.,* BQ) can be generated from the electrochemical conversion of parent pollutants, but it may limit the wide applicability of this suggested approach for water purification to some extent. For instance, the efficiency of electrooxidation would be considerably lowered when the content of aromatic organic pollutants is very low (pg/L-ng/L) in water. Fortunately, thanks to rapid advances in coordination and organic chemistry, one promising idea is to develop quinone-based materials (*e.g.,* quinone loaded carbon nanotubes) to efficiently activate PMS for selective contaminant remediation, which will also simplify the experimental setup and eliminate the cost of electricity. Furthermore, since quinone-like moieties are key components of natural organic matter in soils and waters, our research could be valuable in designing *in situ* remediation strategies for contaminated soil and water.

CRediT authorship contribution statement

Fuqiang Liu: Data curation, Methodology, Investigation, Writing – original draft. **Zhiyuan Wang:** Methodology, Validation. **Shijie You:** Conceptualization, Funding acquisition, Writing – review & editing. **Yanbiao Liu:** Conceptualization, Supervision, Resources, Writing – review & editing.

Declaration of Competing Interest

The authors declare that they have no known competing financial interests or personal relationships that could have appeared to influence the work reported in this paper.

Acknowledgments

This work was supported by the National Natural Science Foundation of China (Nos. 52170068 and U21A20161), the Open Project of State Key Laboratory of Urban Water Resource and Environment, Harbin Institute of Technology (No. QAK202108) and Heilongjiang Touyan Innovation Team Program (HIT-SE-01).

Appendix A. Supplementary material

Supplementary data associated with this article can be found in the online version at doi:10.1016/j.apcatb.2022.121980.

References

[1] B.P. Chaplin, The prospect of electrochemical technologies advancing worldwide water treatment, Acc. Chem. Res. 52 (2019) 596–604, https://doi.org/10.1021/acs.accounts.8b00611.

[2] Y.B. Liu, G.D. Gao, C.D. Vecitis, Prospects of an electroactive carbon nanotube membrane toward environmental applications, Acc. Chem. Res. 53 (2020) 2892–2902, https://doi.org/10.1021/acs.accounts.0c00544.

[3] C. Liu, A.Y. Zhang, Y. Si, D.N. Pei, H.Q. Yu, Photochemical anti-fouling approach for electrochemical pollutant degradation on facet-tailored TiO_2 single crystals, Environ. Sci. Technol. 51 (2017) 11326–11335, https://doi.org/10.1021/acs.est.7b04105.

[4] G.W. Muna, N. Tasheva, G.M. Swain, Electro-oxidation and amperometric detection of chlorinated phenols at boron-doped diamond electrodes: a comparison of microcrystalline and nanocrystalline thin films, Environ. Sci. Technol. 38 (2004) 3674–3682, https://doi.org/10.1021/es034656e.

[5] M. Panizza, G. Cerisola, Direct and mediated anodic oxidation of organic pollutants, Chem. Rev. 109 (2009) 6541–6569, https://doi.org/10.1021/cr9001319.

[6] D.N. Pei, C. Liu, A.Y. Zhang, X.Q. Pan, H.Q. Yu, In situ organic Fenton-like catalysis triggered by anodic polymeric intermediates for electrochemical water purification, Proc. Natl. Acad. Sci. USA 117 (2020) 30966–30972, https://doi.org/10.1073/pnas.2005035117.

[7] X.F. Liu, S.J. You, F. Ma, H. Zhou, Characterization of electrode fouling during electrochemical oxidation of phenolic pollutant, Front. Environ. Sci. Eng. 15 (2021) 53, https://doi.org/10.1007/s11783-020-1345-7.

[8] A.M. Zaky, B.P. Chaplin, Mechanism of p-substituted phenol oxidation at a Ti_4O_7 reactive electrochemical membrane, Environ. Sci. Technol. 48 (2014) 5857–5867, https://doi.org/10.1021/es5010472.

[9] M. Ferreira, M.F. Pinto, L.C. Neves, A.M. Fonseca, O. Soares, J.J.M. Orfao, M.F. R. Pereira, J.L. Figueiredo, P. Parpot, Electrochemical oxidation of aniline at mono and bimetallic electrocatalysts supported on carbon nanotubes, Chem. Eng. J. 260 (2015) 309–315, https://doi.org/10.1016/j.cej.2014.08.005.

[10] R. Berenguer, J.M. Sieben, C. Quijada, E. Morallon, Electrocatalytic degradation of phenol on Pt- and Ru-doped Ti/SnO_2-Sb anodes in an alkaline medium, Appl. Catal. B 199 (2016) 394–404, https://doi.org/10.1016/j.apcatb.2016.06.038.

[11] C.K. Duesterberg, T.D. Waite, Kinetic modeling of the oxidation of p-hydroxybenzoic acid by Fenton's reagent: implications of the role of quinones in the redox cycling of iron, Environ. Sci. Technol. 41 (2007) 4103–4110, https://doi.org/10.1021/es0628699.

[12] G.D. Fang, J. Gao, D.D. Dionysiou, C. Liu, D.M. Zhou, Activation of persulfate by quinones: free radical reactions and implication for the degradation of PCBs, Environ. Sci. Technol. 47 (2013) 4605–4611, https://doi.org/10.1021/es400262n.

[13] K. Xu, H.Y. Dong, M.K. Li, Z.M. Qiang, Quinone group enhances the degradation of levofloxacin by aqueous permanganate: Kinetics and mechanism, Water Res. 143 (2018) 109–116, https://doi.org/10.1016/j.watres.2018.06.026.

[14] E.E. Daugherty, B. Gilbert, P.S. Nico, T. Borch, Complexation and redox buffering of iron(II) by dissolved organic matter, Environ. Sci. Technol. 51 (2017) 11096–11104, https://doi.org/10.1021/acs.est.7b03152.

[15] X.H. Li, W.L. Guo, Z.H. Liu, R.Q. Wang, H. Liu, Quinone-modified NH_2-MIL-101 (Fe) composite as a redox mediator for improved degradation of bisphenol A, J. Hazard. Mater. 324 (2017) 665–672, https://doi.org/10.1016/j.jhazmat.2016.11.040.

[16] J. Liang, X.G. Duan, X.Y. Xu, K.X. Chen, F. Wu, H. Qiu, C.S. Liu, S.B. Wang, X. D. Cao, Biomass-derived pyrolytic carbons accelerated Fe(III)/Fe(II) redox cycle for persulfate activation: pyrolysis temperature-depended performance and mechanisms, Appl. Catal. B 297 (2021), 120446, https://doi.org/10.1016/j.apcatb.2021.120446.

[17] J. Xiao, C. Wang, H. Liu, Fenton-like degradation of dimethyl phthalate enhanced by quinone species, J. Hazard. Mater. 382 (2020), 121007, https://doi.org/10.1016/j.jhazmat.2019.121007.

[18] Y. Zhou, J. Jiang, Y. Gao, S.Y. Pang, Y. Yang, J. Ma, J. Gu, J. Li, Z. Wang, L. H. Wang, L.P. Yuan, Y. Yang, Activation of peroxymonosulfate by phenols: important role of quinone intermediates and involvement of singlet oxygen, Water Res. 125 (2017) 209–218, https://doi.org/10.1016/j.watres.2017.08.049.

[19] J.Q. Ding, H. Nie, S.L. Wang, Y.S. Chen, Y. Wan, J.W. Wang, H.L. Xiao, S.Y. Yue, J. Ma, P.C. Xie, Transformation of acetaminophen in solution containing both peroxymonosulfate and chlorine: performance, mechanism, and disinfection by-product formation, Water Res. 189 (2021), 116605, https://doi.org/10.1016/j.watres.2020.116605.

[20] Y. Zhou, J. Jiang, Y. Gao, J. Ma, S.Y. Pang, J. Li, X.T. Lu, L.P. Yuan, Activation of peroxymonosulfate by benzoquinone: a novel nonradical oxidation process, Environ. Sci. Technol. 49 (2015) 12941–12950, https://doi.org/10.1021/acs.est.5b03595.

[21] H. Zhang, L.N. Qiao, J. He, N. Li, D.M. Zhang, K. Yu, H. You, J. Jiang, Activating peroxymonosulfate by halogenated and methylated quinones: Performance and mechanism, RSC Adv. 9 (2019) 27224–27230, https://doi.org/10.1039/c9ra04789a.

[22] J. Gu, Y. Song, Y. Yang, C.T. Guan, J. Jiang, Mechanical insights into activation of peroxides by quinones: Formation of oxygen-centered radicals or singlet oxygen, Environ. Sci. Technol. 56 (2022) 8776–8783, https://doi.org/10.1021/acs.est.1c08883.

[23] D.L. Guo, Y.B. Liu, H.D. Ji, C.C. Wang, B. Chen, C.S. Shen, F. Li, Y.X. Wang, P. Lu, W. Liu, Silicate-enhanced heterogeneous flow-through electro-Fenton system using iron oxides under nanoconfinement, Environ. Sci. Technol. 55 (2021) 4045–4053, https://doi.org/10.1021/acs.est.1c00349.

[24] B. Barrios, B. Mohrhardt, P.V. Doskey, D. Minakata, Mechanistic insight into the reactivities of aqueous-phase singlet oxygen with organic compounds, Environ. Sci. Technol. 55 (2021) 8054–8067, https://doi.org/10.1021/acs.est.1c01712.

[25] L.S. Zhang, X.H. Jiang, Z.A. Zhong, L. Tian, Q. Sun, Y.T. Cui, X. Lu, J.P. Zou, S. L. Luo, Carbon nitride supported high-loading Fe single-atom catalyst for activating of peroxymonosulfate to generate $^1O_2$ with 100% selectivity, Angew. Chem. Int. Ed. 60 (2021) 21751–21755, https://doi.org/10.1002/anie.202109488.

[26] X.G. Duan, H.Q. Sun, Z.P. Shao, S.B. Wang, Nonradical reactions in environmental remediation processes: Uncertainty and challenges, Appl. Catal. B 224 (2018) 973–982, https://doi.org/10.1016/j.apcatb.2017.11.051.

[27] Y.M. Zhao, M. Sun, X.X. Wang, C. Wang, D.W. Lu, W. Ma, S.A. Kube, J. Ma, M. Elimelech, Janus electrocatalytic flow-through membrane enables highly selective singlet oxygen production, Nat. Commun. 11 (2020) 6228, https://doi.org/10.1038/s41467-020-20071-w.

[28] X. Cheng, H.G. Guo, Y.L. Zhang, X. Wu, Y. Liu, Non-photochemical production of singlet oxygen via activation of persulfate by carbon nanotubes, Water Res. 113 (2017) 80–88, https://doi.org/10.1016/j.watres.2017.02.016.

[29] F. Li, X. Peng, Y.B. Liu, J.C. Mei, L.W. Sun, C.S. Shen, C.Y. Ma, M.H. Huang, Z. W. Wang, W.G. Sand, A chloride-radical-mediated electrochemical filtration system for rapid and effective transformation of ammonia to nitrogen, Chemosphere 229 (2019) 383–391, https://doi.org/10.1016/j.chemosphere.2019.04.180.

[30] Q.Q. Huang, J.Y. Zhang, Z.Y. He, P.H. Shi, X. Qin, W.F. Yao, Direct fabrication of lamellar self-supporting Co_3O_4/N/C peroxymonosulfate activation catalysts for effective aniline degradation, Chem. Eng. J. 313 (2017) 1088–1098, https://doi.org/10.1016/j.cej.2016.11.002.

[31] H.J. Ding, Y. Zhu, Y.L. Wu, J. Zhang, H.P. Deng, H.L. Zheng, Z. Liu, C. Zhao, In situ regeneration of phenol-saturated activated carbon fiber by an electro-peroxymonosulfate process, Environ. Sci. Technol. 54 (2020) 10944–10953, https://doi.org/10.1021/acs.est.0c03766.

[32] F. Ghanbari, M. Moradi, Application of peroxymonosulfate and its activation methods for degradation of environmental organic pollutants: review, Chem. Eng. J. 310 (2017) 41–62, https://doi.org/10.1016/j.cej.2016.10.064.

[33] H.Y. Dong, Y. Li, S.C. Wang, W.F. Liu, G.M. Zhou, Y.F. Xie, X.H. Guan, Both Fe(IV) and radicals are active oxidants in the Fe(II)/peroxydisulfate process, Environ. Sci. Technol. Lett. 7 (2020) 219–224, https://doi.org/10.1021/acs.estlett.0c00025.

[34] F. Chen, L.L. Liu, J.J. Chen, W.W. Li, Y.P. Chen, Y.J. Zhang, J.H. Wu, S.C. Mei, Q. Yang, H.Q. Yu, Efficient decontamination of organic pollutants under high salinity conditions by a nonradical peroxymonosulfate activation system, Water Res. 191 (2021), 116799, https://doi.org/10.1016/j.watres.2020.116799.

[35] L.L. Yang, G.R. Liu, M.H. Zheng, R. Jin, Q.Q. Zhu, Y.Y. Zhao, X.L. Wu, Y. Xu, Highly elevated levels and particle-size distributions of environmentally persistent free radicals in haze-associated atmosphere, Environ. Sci. Technol. 51 (2017) 7936–7944, https://doi.org/10.1021/acs.est.7b01929.

[36] L.M. Jin, S.J. You, X.G. Duan, Y. Yao, J.M. Yang, Y.B. Liu, Peroxymonosulfate activation by Fe_3O_4-MnO_2/CNT nanohybrid electroactive filter towards ultrafast micropollutants decontamination: performance and mechanism, J. Hazard. Mater. 423 (2022), 127111, https://doi.org/10.1016/j.jhazmat.2021.127111.

[37] J. Lee, U. von Gunten, J.H. Kim, Persulfate-based advanced oxidation: critical assessment of opportunities and roadblocks, Environ. Sci. Technol. 54 (2020) 3064–3081, https://doi.org/10.1021/acs.est.9b07082.

[38] C.J. Zhang, H. Chen, G. Xue, Y.B. Liu, S.P. Chen, C. Jia, A critical review of the aniline transformation fate in azo dye wastewater treatment, J. Clean. Prod. 321 (2021), 128971, https://doi.org/10.1016/j.jclepro.2021.128971.

[39] A. Benito, A. Penades, J.L. Lliberia, R. Gonzalez-Olmos, Degradation pathways of aniline in aqueous solutions during electro-oxidation with BDD electrodes and UV/H_2O_2 treatment, Chemosphere 166 (2017) 230–237, https://doi.org/10.1016/j.chemosphere.2016.09.105.

[40] M. Matsushita, H. Kuramitz, S. Tanaka, Electrochemical oxidation for low concentration of aniline in neutral pH medium: application to the removal of aniline based on the electrochemical polymerization on a carbon fiber, Environ. Sci. Technol. 39 (2005) 3805–3810, https://doi.org/10.1021/es040379f.

[41] X.Y. Duan, Y.W. Chen, X.Y. Liu, L.M. Chang, Synthesis and characterization of nanometal-ordered mesoporous carbon composites as heterogeneous catalysts for electrooxidation of aniline, Electrochim. Acta 251 (2017) 270–283, https://doi.org/10.1016/j.electacta.2017.08.118.

[42] Y.G. Bu, H.C. Li, W.J. Yu, Y.F. Pan, L.J. Li, Y.F. Wang, L.T. Pu, J. Ding, G.D. Gao, B. C. Pan, Peroxydisulfate activation and singlet oxygen generation by oxygen vacancy for degradation of contaminants, Environ. Sci. Technol. 55 (2021) 2110–2120, https://doi.org/10.1021/acs.est.0c07274.

[43] H. Chow, A.L.T. Pham, Mitigating electrode fouling in electrocoagulation by means of polarity reversal: The effects of electrode type, current density, and polarity reversal frequency, Water Res. 197 (2021), 117074, https://doi.org/10.1016/j.watres.2021.117074.

[44] Y. Zhang, X.Y. Xu, P.Y. Zhang, L. Zhao, H. Qiu, X.D. Cao, Pyrolysis-temperature depended quinone and carbonyl groups as the electron accepting sites in barley grass derived biochar, Chemosphere 232 (2019) 273–280, https://doi.org/10.1016/j.chemosphere.2019.05.225.

[45] J. Huang, Z.Q. Zhao, T. Chen, Y. Zhu, Z.H. Lv, X. Gong, Y.Y. Niu, B.G. Ma, Preparation of highly dispersed expandable graphite/polystyrene composite foam via suspension polymerization with enhanced fire retardation, Carbon 146 (2019) 503–512, https://doi.org/10.1016/j.carbon.2019.02.029.

[46] F.Q. Liu, Y.B. Liu, A.F. Yao, Y.X. Wang, X.F. Fang, C.S. Shen, F. Li, M.H. Huang, Z. W. Wang, W.G. Sand, J.P. Xie, Supported atomically-precise gold nanoclusters for enhanced flow-through electro-Fenton, Environ. Sci. Technol. 54 (2020) 5913–5921, https://doi.org/10.1021/acs.est.0c00427.

[47] Y.N. Liu, H. Zhang, J.H. Sun, J.X. Liu, X. Shen, J.X. Zhan, A. Zhang, S. Ognier, S. Cavadias, P. Li, Degradation of aniline in aqueous solution using non-thermal plasma generated in microbubbles, Chem. Eng. J. 345 (2018) 679–687, https://doi.org/10.1016/j.cej.2018.01.057.

[48] W.T. Zheng, Y.B.A. Liu, W. Liu, H.D. Ji, F. Li, C.S. Shen, X.F. Fang, X. Li, X.G. Duan, A novel electrocatalytic filtration system with carbon nanotube supported nanoscale zerovalent copper toward ultrafast oxidation of organic pollutants, Water Res. 194 (2021), 116961, https://doi.org/10.1016/j.watres.2021.116961.